

Iron Oxide Filled Magnetic Carbon Nanotube–Enzyme Conjugates for Recycling of Amyloglucosidase: Toward Useful Applications in Biofuel Production Process

Wei Jiang Goh,^{†,‡} Venkata S. Makam,^{†,‡} Jun Hu,^{†,‡} Lifeng Kang,[†] Minrui Zheng,[§] Sia Lee Yoong,[†] Chammika N. B. Udalagama,[§] and Giorgia Pastorin^{*,†,||,⊥}

[†]Department of Pharmacy, National University of Singapore, Science Drive 2, S15#05-PI-03, Singapore 117543

[‡]Institute of Chemical and Engineering Sciences, 1 Pesek Road, Jurong Island, Singapore 62783

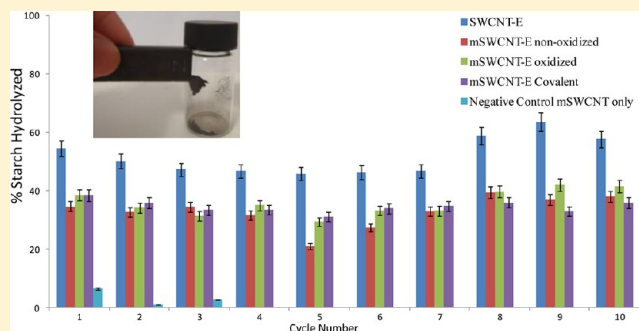
[§]Department of Physics, National University of Singapore, Science Drive 3, Singapore 117542

^{||}NUS Graduate School for Integrative Sciences and Engineering, Centre For Life Sciences (CeLS), 28 Medical Drive, #05-01, Singapore 117456

[⊥]NUSNNI-NanoCore, National University of Singapore, T-Lab Level 11, 5A Engineering Drive 1, Singapore 117580

S Supporting Information

ABSTRACT: Biofuels are fast advancing as a new research area to provide alternative sources of sustainable and clean energy. Recent advances in nanotechnology have sought to improve the efficiency of biofuel production, enhancing energy security. In this study, we have incorporated iron oxide nanoparticles into single-walled carbon nanotubes (SWCNTs) to produce magnetic single-walled carbon nanotubes (mSWCNTs). Our objective is to bridge both nanotechnology and biofuel production by immobilizing the enzyme, Amyloglucosidase (AMG), onto mSWCNTs using physical adsorption and covalent immobilization, with the aim of recycling the immobilized enzyme, toward useful applications in biofuel production processes. We have demonstrated that the enzyme retains a certain percentage of its catalytic efficiency (up to 40%) in starch prototype biomass hydrolysis when used repeatedly (up to ten cycles) after immobilization on mSWCNTs, since the nanotubes can be easily separated from the reaction mixture using a simple magnet. The enzyme loading, activity, and structural changes after immobilization onto mSWCNTs were also studied. In addition, we have demonstrated that the immobilized enzyme retains its activity when stored at 4 °C for at least one month. These results, combined with the unique intrinsic properties of the nanotubes, pave the way for greater efficiency in carbon nanotube–enzyme bioreactors and reduced capital costs in industrial enzyme systems.



1. INTRODUCTION

In an era of escalating demand for energy and the instability in oil producing countries,¹ biofuels provide one of the several alternatives over conventional oil-based energy systems. Coupled with a climate of increasing environmental awareness and deleterious effects of current energy systems on the environment, biofuels possess distinct advantages over oil-based energy systems as they are clean,² renewable, and sustainable, especially with the backdrop of increasing global demand.^{3,4}

The use of enzymes in biofuels is an important step in the overall production process,⁵ as enzymes have several crucial properties such as specificity, use of mild reaction conditions, absence of secondary reactions, as well as reduced energy consumption compared to chemical processes. However, the use of free enzymes poses problems of instability, efficiency, as well as recovery from the substrates. In order to improve the stability of enzymes in solution, attachment to physical

supports such as carbon nanotubes (CNTs) has been explored, because immobilized enzymes tend to show greater stability and hence higher propensity to be reused.^{6,7}

Nanomaterials have been widely studied as a physical support structure for enzymes, because they possess favorable characteristics such as high surface area and effective enzyme loading.^{7,8} From the literature, the nanomaterials studied include nanoparticles, nanofibers, and carbon nanotubes.⁹

Among these, CNTs have gained a growing interest since their development in 1991,^{10,11} mainly due to their favorable physicochemical properties. These include high surface area, unique electronic properties, strong adsorptive ability, and greater affordability over other physical supports.^{12,13} In fact,

Received: July 27, 2012

Revised: November 7, 2012

Published: November 13, 2012

different from other materials (e.g., polymers) that experience aging and alteration of their properties over the time, resulting in increased levels of aldehydes, carboxylates, and peroxides,¹⁴ CNTs present high mechanical, chemical, and thermal stabilities.

Moreover, carbon nanotubes can be functionalized and have been studied extensively, with many potential applications proposed such as drug delivery,¹² biosensors,¹⁵ and biofuel cells.¹⁶ They have also been found to provide excellent support for the differentiation of stem cells¹⁷ and for the immobilization of proteins,^{6–8} improving the physical stability of the enzymes, hence allowing them to be reused.

However, a difficulty faced in the use of enzymes immobilized on CNTs is the dispersion and the subsequent recovery from the reaction mixture for repeated use.¹⁸ Hence, a solution is to render the CNTs magnetic by filling them with magnetic iron oxide nanoparticles,^{18–20} allowing the easy recovery and reuse of the mSWCNT-enzyme conjugates by means of a simple magnet.²⁰

In our study, amyloglucosidase (AMG) was selected as model of enzyme to effectively hydrolyze starch that represented our biomass prototype, a precursor step for the biomass-to-biofuel production process. Amyloglucosidase contains high threonine and serine amino acids (equivalent to about 10% and 13% of the total amino acid content, respectively), while it does not contain any sulfur-containing amino acids. This enzyme is normally combined with other enzymes (e.g., pectinase) or as enzyme complex, in order to maximize the amount of ethanol formation from starch.²¹ Indeed, amyloglucosidase and pectinase have been shown to be the most effective enzymes in terms of amylase activity and ethanol production.²² Additional advantages include low cost, commercial availability, and sufficient purity for their use in the starch digest method. Moreover, since AMG is commonly used in studies dealing with ethanol production,^{23–25} it represented a good choice for the evaluation of starch hydrolysis either in the form of free enzyme or as enzyme immobilized onto a substrate (i.e., carbon nanotubes).

Finally, the ability of the immobilized enzymes to be recovered and reused is pertinent in industrial biofuel systems, because it would result in greater efficiency and therefore defray production costs, thus deriving economic benefits. By immobilizing AMG onto the mSWCNTs, we could demonstrate the recovery of the immobilized enzyme on a magnet, and subsequently reuse the mSWCNT-AMG complex several times.

2. EXPERIMENTAL SECTION

2.1. Materials. CNTs with 90% purity (purity of SWCNTs > 50%) were purchased from Shenzhen Nanotech Port Co. Ltd. (China). As reported by the manufacturer, they consisted of a mixture of single- and double/multiple-walled CNTs with diameters between <1 and 5 nm. Aqueous solution of Amyloglucosidase (≥ 300 U/mL) from *Aspergillus niger* was purchased from Sigma Aldrich and used without further purification. Bicinchoninic acid (BCA) assay reagents were purchased from Pierce Biotechnology Inc. (Rockford, USA). Ammonium iron(II) sulfate hexahydrate (99%) was purchased from Alfa Aesar China. All other reagents were purchased from Sigma Aldrich and used as received.

UV circular dichroism data were obtained using a Jasco J-810 spectropolarimeter. Absorbance measurements were taken using a Magellan Tecan plate reader (version 6.6).

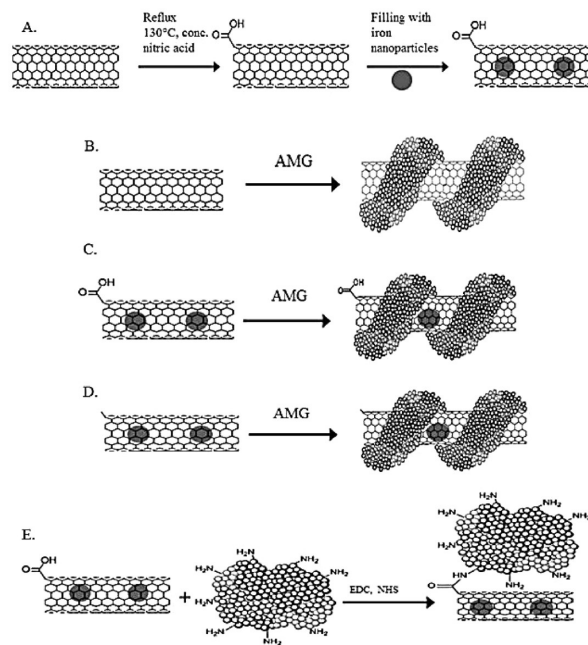
2.2. Production of Magnetic SWCNTs (mSWCNTs). SWCNTs were filled with Fe₃O₄ using a simple method adapted from Li et al.²⁶

In this method, 5 mg of SWCNTs was oxidized under reflux at 130 °C for 15 min in 65% nitric acid solution. The oxidized SWCNTs were filtered, and washed with water till the filtrate was neutral. This oxidation step was omitted in the production of magnetic non-oxidized iron oxide filled SWCNTs.

0.15 g of ammonium iron(II) sulfate hexahydrate was dissolved in 5 mL of deionized (DI) water and hydrazine hydrate solution in a volume ratio of 3:1 to achieve a dark green solution. The oxidized SWCNTs were then added to the solution. The mixture was then sonicated and stirred vigorously for 24 h and the pH adjusted to 11–13 using ammonia solution to facilitate the uptake of the iron solution into the SWCNTs. The surface of SWCNTs was cleaned from iron oxide solution by reacting the tubes with diluted hydrochloric acid and then rinsing them with ethyl acetate.

In order to produce solid Fe₃O₄ nanoparticles in the SWCNTs, the above mixture was refluxed at 130 °C for 2 h in chlorobenzene, following which it was filtered, washed with dimethylformamide, ethanol, and finally DI water. To clean the surface of the SWCNTs of any Fe₃O₄ nanoparticles, the mSWCNTs were washed with dilute hydrochloric acid and then rinsed with ethyl acetate and DI water while filtering. Lastly, the SWCNTs were suspended in DI water and freeze-dried for 24 h to obtain mSWCNTs, as shown in Scheme 1a. The mSWCNTs were tested to be able to be attracted by a simple magnet (Figure S2 in Supporting Information).

Scheme 1. Preparation of mSWCNT-AMG Complexes



(A) Encapsulation of pristine SWCNT with magnetic iron oxide nanoparticles. (B) Physical adsorption of AMG enzyme onto pristine SWCNT. (C) Physical adsorption of AMG enzyme onto oxidized mSWCNT. (D) Physical adsorption of AMG enzyme onto non oxidized mSWCNT. (E) Covalent immobilization of AMG enzyme onto mSWCNT via carbodiimide chemistry.

2.3. Physical Adsorption of AMG. Physical adsorption of the enzyme AMG was done on pristine SWCNTs, non-oxidized mSWCNTs, and oxidized mSWCNTs, as shown in Scheme 1b,c and d. Briefly, 2 mg of SWCNTs of each type were dispersed in 1 mL of dimethylformamide, filtered, and then resuspended in 950 μ L of acetate buffer (50 mM, pH 5.5) to clean and better disperse them. The SWCNTs/mSWCNTs were then sonicated for 0.5 h until an even dispersion was obtained. 50 μ L of AMG enzyme was then added to the samples and kept at 4 °C in an ice bath for 2 h (Scheme 1B,C). The samples were then centrifuged at 6000 rpm for 10 min for 4 cycles,

collecting the supernatant for BCA assay and resuspending the pellet in fresh acetate buffer each time. In order to ensure maximum enzyme loading, a slight excess of AMG enzyme was used.

2.4. Covalent Immobilization of AMG on Oxidized mSWCNTs by Carbodiimide Chemistry. Two milligrams of mSWCNTs were oxidized as described earlier. The oxidized mSWCNTs were then dispersed and sonicated in 1 mL of 2-(*N*-morpholino)ethanesulfonic acid (MES) buffer (50 mM, pH 6.2) and 1 mL of *N*-hydroxysuccinimide (NHS) (400 mM) for 30 min. After which, *N*-ethyl-*N'*-(3-dimethylaminopropyl)carbodiimide hydrochloride (EDC) was added to initiate the coupling of NHS to the carboxylic groups on the oxidized mSWCNTs. The mixture was allowed to mix for 30 min, then filtered and washed with MES buffer and DI water to remove any unreacted reagent. The mSWCNT film was then transferred to a solution containing 950 μL of acetate buffer and 50 μL of AMG. The mSWCNT film was sonicated to dislodge the nanofilm and mix it uniformly. The AMG was allowed to bind by covalent immobilization for 1 h at 4 °C in an ice bath as shown in Scheme 1e. The mixture was then centrifuged four times at 6000 rpm for 10 min each, collecting the supernatant and resuspending the pellet in fresh acetate buffer each time to remove any unbound enzyme. Similarly, a slight excess of AMG enzyme was used in order to ensure maximum enzyme loading.

2.5. Quantification of Enzyme Loading by BCA Assay. The supernatants from each immobilization method were collected and used in the BCA assay to determine the mass of enzyme on 1 mg of SWCNTs/mSWCNTs. This was done by subtracting the amount of enzyme determined by the BCA assay in the supernatant from the total amount of enzyme added to the CNTs.

2.6. Enzyme Activity by Starch Assay. The activity of AMG was determined by using starch as the substrate, since AMG hydrolyzes starch to glucose through an adaptation of the Fuwa method.^{27,28} In the starch assay, starch solutions of known increasing concentrations diluted in acetate buffer (50 mM, pH 5.5) were prepared in a total volume of 500 μL . Fixed concentrations of 30 μL of AMG or AMG immobilized by the different immobilization methods were added to each starch dilution. After reacting for 5 min, the reaction was stopped by addition of 50 μL of 50% trichloroacetic acid, followed by 100 μL of iodine reagent (0.2% iodine and 2% potassium iodine). Iodine reacted with any remaining starch to give a starch–iodine complex and the absorbance was measured at 590 nm.

2.7. Transmission Electron Microscopy (TEM). SWCNT samples were examined by transmission electron microscopy (TEM) using a JEOL JEM 2010F microscope. The samples were prepared on 200 mesh copper grids coated with Formvar. Length and diameter measurement calculations, based on microscopic scale, were performed using *Image J* software (U.S. National Institute of Health).

2.8. FTIR, ICP-OES, and Raman Analysis. FTIR experiments (0.2 mg on KBr disc) were performed using a Perkin-Elmer Spectrum100 FT-IR Spectrometer (data not shown).

Thermogravimetric analysis (TGA) and determination of Fe levels using ICP-OES Optima 5300 DV (Perkin-Elmer) were performed by CMMAC (NUS) (Supporting Information). The samples were heated in air at a rate of 10 °C/min until a final temperature 1000 °C was reached. After that, they were digested with HNO_3/HCl and top up to 10 mL with H_2O .

MicroRaman spectroscopy was carried out using a Renishaw inVia confocal Raman microscope with an excitation wavelength of 532 nm and a low laser intensity of 0.5 W focused onto the nanotubes using a 50 \times lens.

2.9. Lennard-Jones Potential. This calculation was performed to identify the diameter of the nanotubes that were able to suck a Fe_3O_4 nanoparticle approaching the tip of the tube. In this experiment, Fe_3O_4 nanoparticles were assumed of 2–3 nm in radius (as observed from the TEM images), with a surface atomic density of 0.081 72 per square angstrom. The C–Fe constants were calculated from previously reported data.²⁹ Carbon nanotubes were modeled as an averaged atomic mass distributed over the surface of an open semi-infinite cylinder.

2.10. Gel Electrophoresis (SDS-PAGE). Sodium dodecyl sulfate polyacrylamide gel electrophoresis (SDS-PAGE) was performed in order to further elucidate the presence of enzyme conjugates on the carbon nanotubes using the various immobilization methods. The gel was then stained with Coomassie Brilliant Blue stain for 24 h and destained using acetic acid to visualize the separated enzymes (Supporting Information).

2.11. Circular Dichroism Spectroscopy (CD). Circular dichroism spectroscopy was used to determine the change in α and β conformation from the various enzyme immobilization methods. All samples were diluted to 20 $\mu\text{g}/\text{mL}$ using acetate buffer (10 mM, pH 5.5). The AMG enzyme was diluted 1:500 with 10 mM acetate buffer.

2.12. Repeated Use of AMG Enzyme on mSWCNTs Using Different Immobilization Methods. 100 μL of 2 mg/mL mSWCNTs with AMG immobilized by the various methods (as described previously) were added to 200 μL of 100 $\mu\text{g}/\text{mL}$ starch substrate and allowed to react for 5 min. The mSWCNT–AMG conjugates were then removed by a simple magnet and 50 μL of 50% trichloroacetic acid was added to stop the reaction. 50 μL of iodine reagent (0.2% iodine and 2% potassium iodine) was then added to form a starch–iodine complex, and the absorbance was measured at 590 nm. The mSWCNT–AMG conjugates were then added to 200 μL of fresh starch substrate for a total of 10 cycles. For the negative control, only mSWCNTs were used. Results were presented from triplicates.

2.13. Stability Study. The stability of the AMG enzyme immobilized onto various surfaces and different immobilization strategies was evaluated with respect to two temperatures, 4 °C and room temperature, over a period of one month. Thirty microliter aliquots of each sample at various time points were added to 100 μL of 100 $\mu\text{g}/\text{mL}$ starch solution. The reaction was stopped and the percentage of starch hydrolyzed was determined by measuring the absorbance at 590 nm. All immobilized enzymes were kept suspended in 50 mM acetate buffer.

3. RESULTS AND DISCUSSION

The immobilization of enzymes on physical supports has been studied extensively in previous works.^{28,30,31} In this aspect, immobilized enzymes pose several advantages over their free, soluble counterparts, including greater physical stability, easy separation from the reaction mixture (thus reducing impurities in the final product), and ability to be reused, thereby reaching higher productivity. Among these immobilization methods, incorporation of enzymes onto a magnetic support is a particularly attractive option as it allows the immobilized enzymes to be separated easily from the reaction mixture by use of a simple magnet with minimum loss of the product, unlike other separation techniques such as filtration and centrifugation. The immobilized enzymes may also be directed by an external magnetic field to achieve greater mixing efficiencies in the reaction mixture.

In this study, physical adsorption and covalent immobilization of the AMG enzyme were performed to examine the effect of different immobilization methods on magnetic carbon nanotubes. The interacting force in the physical adsorption of AMG onto the SWCNTs is primarily via hydrophobic interactions between the hydrophobic regions of the enzyme with the SWCNTs' exterior side walls that are made up of aromatic rings.⁷ As the SWCNTs can be filled with iron oxide nanoparticles with or without an oxidation step, physical adsorption of AMG enzyme was done on both oxidized and nonoxidized SWCNTs. This method consists of simple deposition of the enzyme onto the tubes and it does not involve additional reagents, sequential steps, or enzyme modifications that could affect its activity. Immobilization through adsorption is attractive through its simplicity and its

Table 1. Enzyme Loading, Kinetics, and Structural Changes of Various AMG Enzyme Immobilization Methods

sample name	immobilization method	enzyme loading (mg of AMG enzyme/mg of SWCNTs)	enzyme kinetics		circular dichroism	
			V_{\max}/K_m ($\text{mg}^{-1} \text{s}^{-1}$)	catalytic efficiency (%)	α helices (%)	β sheets (%)
Amyloglucosidase	-	-	1.7323	-	83.7	1.3
A SWCNT-AMG (nonoxidized)	physical adsorption	1.699	0.9944	57.4	4.4	44.2
B mSWCNT-AMG (nonoxidized)	physical adsorption	1.677	0.7272	42.0	4.4	44.2
C mSWCNT-AMG (oxidized)	physical adsorption	1.692	0.6340	36.6	11.5	28.4
D mSWCNT-AMG (oxidized)	covalent immobilization	2.419	0.3673	21.2	11.5	28.4

potential for reversibility, without previous chemical modification of the enzyme. On the other hand, in the covalent approach, the enzyme is irreversibly conjugated through the functional groups present on the tube walls; in this other method, carbodiimide chemistry was used to link the enzyme onto the magnetic CNTs.^{7,32}

The immobilization of the AMG enzyme using various immobilization strategies onto the following CNTs was studied: pristine single-walled carbon nanotubes (SWCNTs), magnetic oxidized carbon nanotubes filled with iron oxide nanoparticles (mSWCNT-AMG oxidized) and magnetic non-oxidized carbon nanotubes filled with iron oxide nanoparticles (mSWCNT-AMG nonoxidized).

3.1. Enzyme Loading by BCA Assay. As observed from Table 1, various immobilization methods of the AMG enzyme (also confirmed by gel electrophoresis (SDS-Page), Figure S1) on different types of CNTs showed that the enzyme loading via physical adsorption yielded approximately similar enzyme loading of 1.7 mg of AMG enzyme per 1 mg of CNTs, whether or not the surface had been modified by oxidation (sample C versus sample B) or if the interior was filled with iron oxide nanoparticles (sample A versus sample B). In contrast, the covalent approach using carbodiimide chemistry (sample D) yielded a much higher enzyme loading of 2.4 mg of AMG enzyme per 1 mg of CNTs. These findings coincide with the expected results as the covalent approach is more specific than physical adsorption, providing extra sites for attachment in addition to physical adsorption, thereby leading to higher AMG enzyme loading.

3.2. Enzyme Kinetics. A more accurate assessment of the changes in the AMG enzyme after immobilization would be to examine the differences in enzyme kinetics. This is done by adding a predetermined concentration of the enzyme AMG conjugates to known concentrations of starch solution. The AMG enzyme hydrolyzes starch to glucose, and iodine can be added to form a starch–iodine complex after a preset time of 5 min to determine the amount of starch left by measuring its absorbance at 590 nm. By using the Michaelis–Menten equation shown in eq 1, we are able to determine the enzyme kinetics of the AMG enzyme conjugated onto the various carbon nanotubes.

$$V_0 = [S] \times V_{\max} / ([S] + K_m) \quad (1)$$

where V_0 is the initial rate of reaction and $[S]$ is starch concentration. V_{\max} represents the maximum rate of reaction reached, and K_m is the concentration term corresponding to half V_{\max} .

As the starch concentration used in the study is relatively small, we can rearrange the Michaelis–Menten equation into a

simple linear form as shown in eq 2, where the gradient would represent the ratio of V_{\max}/K_m . Since the enzyme activity may be expressed as a ratio of V_{\max}/K_m , we are able to directly compare the enzyme activity of the immobilized AMG enzyme when different immobilization strategies are employed, with a greater magnitude of V_{\max}/K_m indicating greater enzyme activity (Table 1).

$$V_0 = [S] \times (V_{\max}/K_m) \quad (2)$$

Also, we noted the V_{\max}/K_m ratio for physical adsorption of enzyme onto nonoxidized and oxidized mSWCNTs was similar (sample B versus sample C). However, the enzyme activity of the nonoxidized mSWCNTs was slightly higher than the one in oxidized mSWCNTs. This may be due to the surface of the nonoxidized mSWCNTs sharing a closer resemblance to the pristine SWCNTs; hence, the degree of conformational change in the enzyme structure after physical adsorption would be expected to be similar to the immobilized enzymes on pristine SWCNTs (sample A), thus resulting in higher enzyme activity compared to the physically adsorbed enzymes on the oxidized mSWCNTs (sample C).

Another parameter of enzyme kinetics is the catalytic efficiency of the immobilized enzyme with respect to the native free AMG enzyme. This would indicate the extent of enzyme activity retained by the AMG enzyme after different enzyme immobilization methods. As seen in Table 1, the catalytic efficiency, as given by the V_{\max}/K_m ratio, has decreased after immobilization onto both pristine SWCNTs and mSWCNTs. This is expected, as immobilization of the AMG enzyme would induce changes in the enzyme conformation, thus reducing the enzyme activity. Notably, the enzyme activity after covalent immobilization is much lower than the other immobilization methods, as seen from its low V_{\max}/K_m ratio. Hence, we deduce that the increased enzyme loading in covalent immobilization (as described earlier) is offset by a greater change in the enzyme conformation, therefore resulting in reduced catalytic activity.

Moreover, it seems that the catalytic activity of the enzyme decreased in the case of all the magnetic samples. It could be that the pretreatment of the tubes with a 70% solution of nitric acid, aimed to minimize the iron oxide adsorbed on the external walls of the SWCNTs, interfered also with the ability of the enzyme to wrap around the tubes and thus with its activity. An alternative explanation could be derived from previous studies^{33,34} demonstrating that the enzyme activity using magnetic particles showed a proportional increase with increasing magnetic properties. The authors concluded that the presence of these magnetic particles affected the catalytic cycle of the enzyme, changing the overall reaction rate.

Therefore, it could be that the magnetization of our nanotubes affected the efficiency of the enzyme. Future studies will be aimed at assessing how the extent of magnetization influences the activity of immobilized enzymes. We could also observe that the V_{\max}/K_m ratio decreased after immobilization in comparison to the free native AMG enzyme, resulting in a reduction of the enzyme activity (Figure 1). Therefore, we

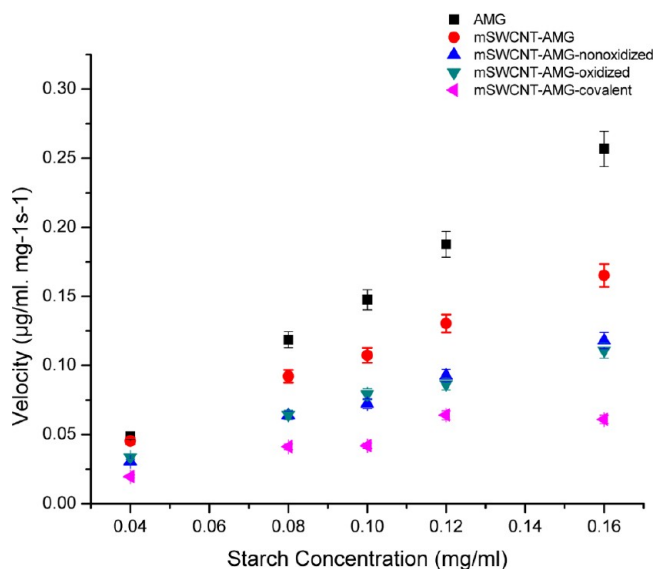


Figure 1. Michaelis–Menten plot of increasing starch concentrations against the rate of reaction.

postulated that the immobilization of the enzyme onto carbon nanotubes resulted in alterations to the conformation and also to the active site of the AMG enzyme, accounting for its reduced activity after immobilization.^{31,35}

3.3. Characterization of SWCNT Samples through Microscopy, FTIR, ICP-OES and Raman Analysis. Oxidized and nonoxidized magnetic SWCNTs were observed under TEM to check the eventual presence of Fe_3O_4 nanoparticles on the surface of mSWCNTs (Figure 2). As can be seen from

Figure 2a,b, pristine SWCNTs appeared as bundles of about 20–50 nm, and there was no obvious difference between tubes that underwent magnetic treatment and those without Fe_3O_4 . We noticed the presence of a few sporadic nanoparticles both inside and outside the nanotube bundles (Figure 2b,c): they most likely consisted of bigger Fe_3O_4 nanoparticles that were not able to enter the small-diameter CNTs and escaped from the washing steps. Interestingly, an enlarged image of a double-walled CNTs (diameter of about 5 nm) found in this sample clearly showed the presence of Fe_3O_4 inside their inner cavity (Figure 2d) in the form of black nanoparticles. More conclusive images were obtained in the case of oxidized mSWCNTs, which clearly showed black Fe_3O_4 dots only inside the tube bundles, while extensive washings were able to remove those unspecifically adsorbed on the external walls of the CNTs (Figure 2e). This result might be a consequence of the shorter length of oxidized mSWCNTs (image not shown), which were more efficient at incorporating Fe_3O_4 nanoparticles in comparison to their pristine longer counterparts.

This was also in agreement with the images proposed by Li and collaborators,²⁶ who suggested that the treatment of CNTs with nitric acid before the encapsulation with Fe_3O_4 nanoparticles rendered their surfaces slippery and thus unwilling to adsorb the nanoparticles on the tubes' sidewalls.

The interaction energy between our SWCNTs and Fe_3O_4 nanoparticles was investigated using the Lennard-Jones potential. This is based on the work done by Baowan et al.³⁶ on TiO_2 nanospheres that uses the formalism of Cox et al.³⁷ where they studied the mechanism of an atom or fullerene molecule being accepted into a CNT by virtue of only the van der Waal interactions. Using the parameters from Mayo et al.,²⁹ we calculated how the suction energy³⁷ for a 30 Å Fe_3O_4 nanosphere varies with the radius of the CNTs. The radius of 30 Å was chosen as a representative radius for the 2–4 nm radii distribution of the nanospheres estimated from the TEM images in Figure 2. In our case, we found that the most favorable suction energy occurs when the nanotube radius is equal to 33.35 Å (Figure 3). Hence, it is at this radius that the Fe_3O_4 nanosphere is imparted the greatest inward, axial velocity

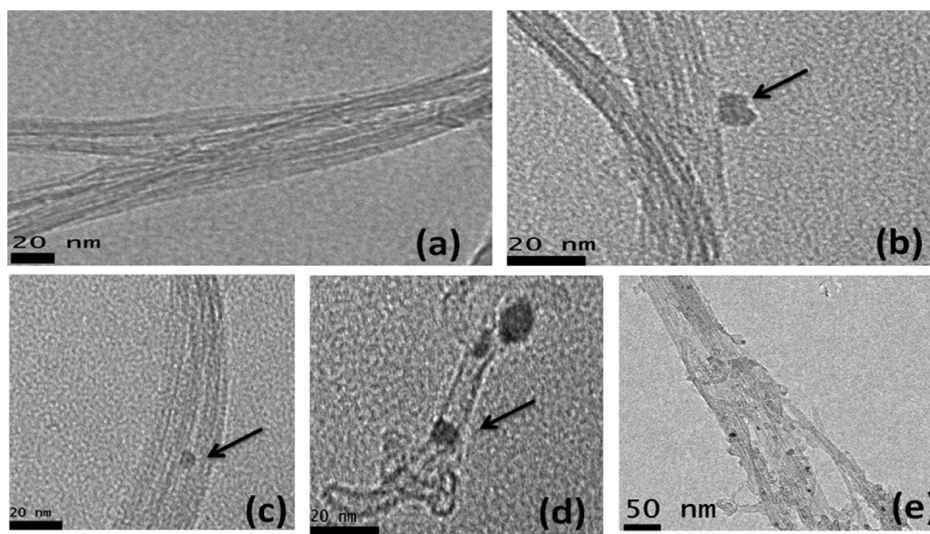


Figure 2. TEM images of SWCNTs: (a) pristine SWCNTs as bundles of 20–50 nm; pristine mSWCNTs with a few Fe_3O_4 nanoparticles outside (b) or inside (c) the bundles; (d) enlarged image of a double/multiwalled CNT showing Fe_3O_4 nanoparticles in the inner cavity; (e) oxidized mSWCNTs showing several Fe_3O_4 nanoparticles.

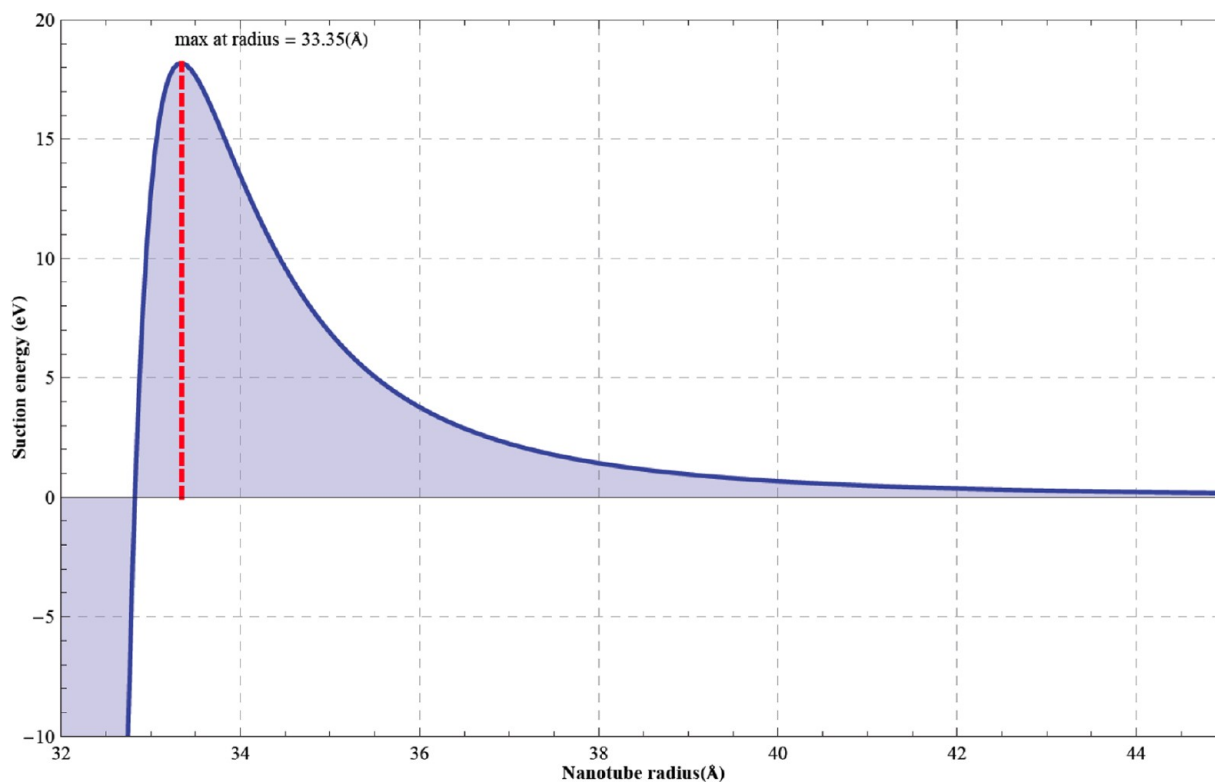


Figure 3. Suction energy for a Fe_3O_4 nanoparticle (radius $a = 30 \text{ \AA}$) inside a SWCNT.

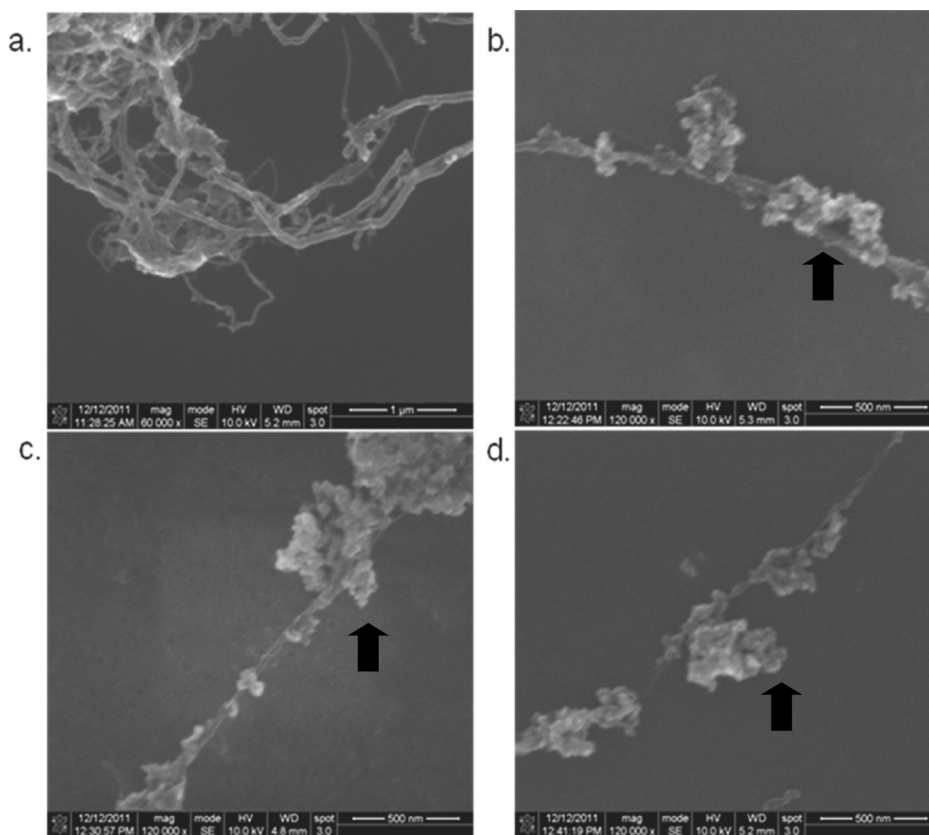


Figure 4. SEM images of (a) pristine carbon nanotubes, (b) AMG adsorbed mSWCNT (oxidized) by physical adsorption, (c) AMG adsorbed mSWCNT (nonoxidized) by physical adsorption, and (d) AMG immobilized mSWCNT (oxidized) by covalent bonding. The globular structures (arrows) are suggestive of AMG enzyme loading.

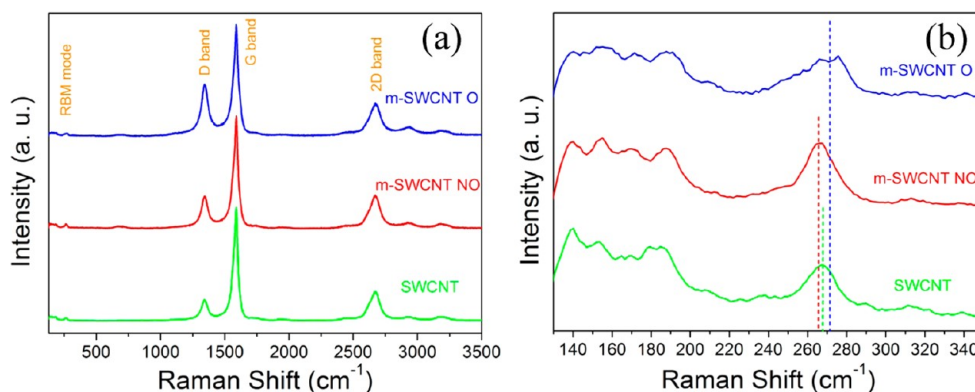


Figure 5. (a) Full-range survey spectra of SWCNTs and variants (blue graph, mSWCNTs Oxidized; red graph, mSWCNTs Nonoxidized; green graph, pristine, nonmagnetic SWCNTs), showing the characteristic G band, D band, and RBM mode. (b) Fine spectra of RBM mode of SWCNTs and variants.

upon being admitted into the CNT and therefore most successfully encapsulated within the potential well of the CNT. Consequently, our SWCNTs of 2–5 nm represent suitable dimensions for the Fe_3O_4 encapsulation to occur (Figure 3). Moreover, the uptake of the iron solution into the SWCNTs was further facilitated through a vigorous sonication and stirring step for at least 24 h to keep the Fe_3O_4 nanoparticles as small as possible.

Moreover, in order to elucidate the presence of the AMG enzyme on the CNTs, SEM was also performed. The samples consisted of single-walled carbon nanotubes (SWCNTs) and a few double/multiwalled carbon nanotubes with size distribution between <1 and 5 nm. Under SEM, it was observed that some of these tubes were larger than 2 nm (as it might appear from Figure 4) while some others were smaller. This could be due to the fact that the tubes existed as bundles of 20–50 nm in diameter (as confirmed by TEM), which might justify the wider dimension in SEM images.

From Figure 4, the globular structures on the mSWCNTs are suggestive of AMG immobilization onto SWCNTs in the form of sphere-like particles on uniform tubes. The fact that AMG appears as aggregates is in full agreement with previously reported SEM images,³⁸ showing analogous structure of enzymes wrapped onto the nanotubes. Nevertheless, the immobilization of the enzyme onto our magnetic nanotubes was never associated with precipitation of the samples: mSWCNT-AMG conjugates remained stable throughout the duration of the experiments, including those assessing the enzyme stability over a period of one month. This might be explained by the AMG presenting a carbohydrate content of around 13% that, if sufficiently exposed, might have imparted a hydrophilic solubilizing effect to our samples.

Also, from the FTIR analysis performed before and after enzyme loading (figure not shown) and in agreement with data available from literature,³⁹ the spectrum showed a broadening of the bands at 3470 cm^{-1} due to H-bonding between NH_2 of AMG and COOH of oxidized CNTs (this was not visible in the case of pristine SWCNTs). In addition, a shift of the carbonyl peak at around $1630\text{--}1690\text{ cm}^{-1}$ was observed. Finally, some changes were visible between 1300 and 950 cm^{-1} , thus confirming the successful incorporation of the enzyme in SWCNT-AMG conjugates. However, due to the fact that carbon nanotubes display a strong optical density in the whole range from 400 cm^{-1} to 4000 cm^{-1} , very diluted samples were

used, thus affecting the quality of the signals in the infrared spectrum.

In addition, TGA followed by ICP-OES analysis was performed to determine the whole iron content. The results indicated that iron in our mSWCNT sample was 330.1 ppm (0.03%) in comparison with 0.30 ppm in the case of pristine SWCNTs (Supporting Information). This confirmed that mSWCNTs did differ from the pristine ones in terms of iron content, and they were magnetic.

In order to further characterize our samples, we conducted a Raman analysis. Besides the D and G bands, associated with the sp^3 -hybridized carbon atoms in the CNTs, SWCNTs show the characteristic radial breathing mode (RBM, below 350 cm^{-1}), which has been demonstrated to be in a strong relationship with the diameter of the nanotubes.^{40,41} As anticipated, the Raman spectrum of mSWCNTs with the incorporation of Fe_3O_4 nanoparticles (Figure 5a) clearly indicated that the peaks of the D and G bands were almost not affected. In other words, there was no peak shift when the SWCNTs underwent Fe_3O_4 encapsulation, indicating that the encapsulation process did not disrupt the C–C bonding arrangement on the SWCNT surfaces. However, the relative peak height of the D band increased from pristine to oxidized CNTs. Indeed, the oxidation step causes the conversion of sp^2 -hybridized carbons into sp^3 -hybridized carbons by introducing carboxylated functions and defects in the honeycomb lattice.

On the contrary, the RBM fine scan spectra indicated that the magnetization process of both nonoxidized and oxidized SWCNTs induced a peak shift in comparison with pristine CNTs. In detail, the peak in the RBM region of pristine SWCNTs at 267.5 cm^{-1} (Figure 5b), which was supposed to be correlated with CNTs showing diameters of 0.909 nm, shifted to 266 cm^{-1} in nonoxidized samples and to 270 cm^{-1} in oxidized CNTs after loading of Fe_3O_4 nanoparticles. Once again, these results confirmed the presence of Fe_3O_4 nanoparticles inside mSWCNTs (rather than on the external walls).

3.4. Circular Dichroism Spectroscopy (CD). CD analysis was conducted to demonstrate the structural changes in the AMG enzyme after immobilization. CD analysis is considered more accurate, as the protein remains in its aqueous environment during the analysis, and thus can be used to correlate to its activity. From Table 1, we were able to observe that the changes in the α helices (%) and β sheets (%) were similar for physical adsorption of the AMG enzyme on pristine carbon nanotubes and magnetic iron oxide filled nonoxidized

carbon nanotubes. This was not surprising as the surfaces for these two types of CNTs are similar, resulting in the same structural changes of the adsorbed enzyme. The structural changes for the AMG immobilized onto the mSWCNTs by physical adsorption and covalent approach are also similar, probably because both surfaces involve carboxylic groups in the enzyme immobilization, thus resulting in similar structural changes.

The relative structure change (%) of all samples, calculated based on the mean residue ellipticity at 218 nm (θ_{218}), gave a reading of 37.2–37.5%. In general, immobilization of the AMG enzyme resulted in a decrease in α helix structure and an increase in β sheet structure, as shown in Figure 6. The

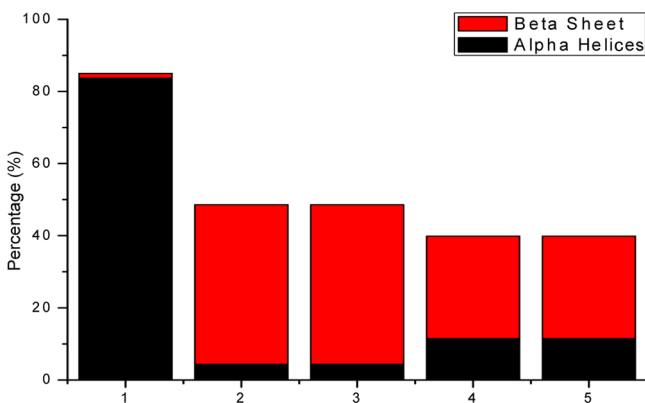


Figure 6. Circular dichroism spectroscopy indicating % of α helices and β sheets: (1) AMG, (2) SWCNT-AMG (physical adsorption), (3) nonoxidized mSWCNT-AMG (physical adsorption), (4) oxidized mSWCNT-AMG (physical adsorption), and (5) oxidized mSWCNT-AMG (covalent immobilization).

decrease in α helix structure was more upon immobilization onto pristine SWCNTs surfaces than oxidized SWCNTs surfaces, and the increase in β sheet structure was observed to be greater in pristine SWCNTs than in the oxidized SWCNTs. It has been proposed that the β -sheet formation leads to a partial destabilization of the secondary and tertiary structures of the protein and an additional exposure of the hydrophobic tryptophan residues to the surface of the enzyme-support complexes.⁴² The enzyme's activity has shown to be highly correlated with tryptophan residues that, upon oxidation, gradually decrease the enzyme's ability to hydrolyze starch. In that case, we would have expected lower enzyme activity in nonoxidized samples due to their higher β -sheet formation (Table 1). Conversely, enzyme kinetics showed a better profile of nonoxidized CNTs in comparison with oxidized samples, thus disproving that particular amino acids were involved in the enzyme's decreased activity. Moreover, it should be noted that amyloglucosidases purified from different sources sometimes differ in terms of their mode of actions on starch.⁴³ This means that the exact amino acids involved in the enzyme activity might be different for amyloglucosidase extracted from *Aspergillus niger* versus *Termitomyces clypeatus*. For that reason, we could not discuss the effect of amino acid content on the activity of AMG enzyme and we could only infer that the surface chemistry of the carbon nanotubes plays an important role in the subsequent immobilized enzyme activity, as it affects how the enzyme would change in its conformation when it is immobilized onto the carbon nanotubes surface.

3.5. Recycling of Immobilized AMG Enzyme. Recycling of immobilized enzymes is a highly relevant application to the biofuel production industry, as enzymes incur fixed costs in production lines. In Figure 7, ten cycles illustrating the

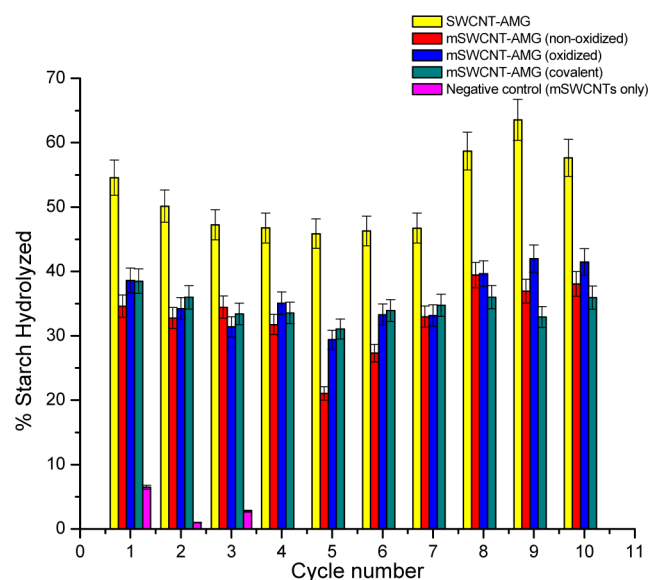


Figure 7. Ten cycles of enzyme recycling using a simple magnet and subsequent reuse of immobilized AMG enzyme onto nonoxidized mSWCNTs and oxidized mSWCNTs by physical adsorption and on oxidized mSWCNT by covalent immobilization. A negative control using only mSWCNTs with no immobilized enzymes was used.

enzymatic activity of immobilized AMG enzymes after recovery by a simple magnet and its subsequent reuse in fresh starch substrate are shown. The fact that our SWCNTs were magnetic and could be collected from the starch solution after repeated usage suggests that the adopted protocol, previously proposed by Li et al. for bigger multiwalled carbon nanotubes, was appropriate even for our smaller tubes.

In each cycle, the percentage of starch hydrolyzed in each cycle for the immobilized AMG onto mSWCNTs remained relatively constant, in the range of 30–40%.

Since immobilized enzymes possess greater physical stability, the decrease in enzymatic activity compared to the native free AMG enzyme is compensated by the ability of the immobilized enzymes on mSWCNTs to be reused. Therefore, the amount of enzyme required to process the starch solution could be decreased: it was estimated that 7.56 mg/mL of free AMG or 3.4 mg of immobilized (not covalently) AMG/mL were necessary to process 50 mM starch, in comparison with a 10-fold lower concentration in the case of recycled enzyme. Indeed, since the percentage of starch hydrolyzed by the immobilized AMG on mSWCNTs remained relatively constant (~35%), the total starch processed by 3.4 mg of immobilized AMG after 10 cycles was about 60 g. The same amount of starch would have required 26.46 g of free AMG, which is almost 8 times higher.

Alternatively, in order to reach the same catalytic end point as the native free AMG enzymes, the amount of immobilized enzymes can be increased, or simply allowed to act on the starch substrate for a longer period of time. Therefore, the ability of the immobilized AMG enzymes to be reused can offset the decrease in activity in the long term, and could result

in potentially substantial cost savings in the biofuel production industry.

3.7. Stability Studies. Stability of a product is an important consideration in the estimation of its shelf life, and can affect its feasibility for use in the biofuel industry. The activity of the immobilized AMG enzymes should be stable for a reasonable period of time, sufficient for transportation and brief storage before use in the bioreactor. Hence, the stability of the AMG enzyme immobilized by the different immobilization methods was assessed over a period of one month (Figure 8).

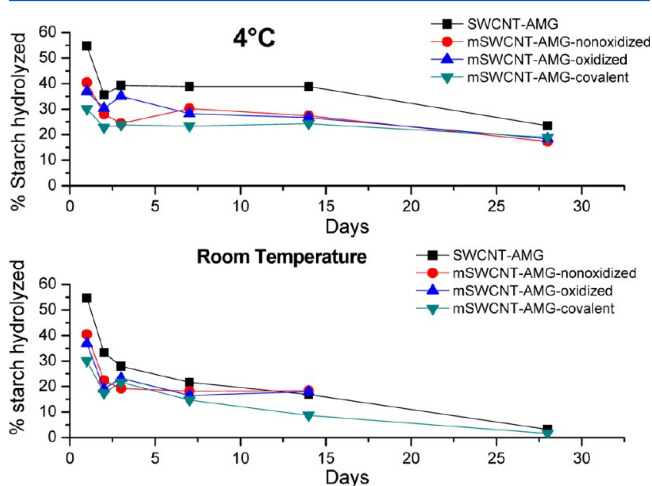


Figure 8. Stability of the AMG enzyme immobilized by physical adsorption and covalent immobilization at 4 °C (top) and at room temperature (bottom) over 28 days, expressed as the percentage of starch hydrolyzed in 5 min.

From Figure 8, it is evident that the activity of the enzyme was more stable when stored at 4 °C than at room temperature, with the enzyme stored at 4 °C maintaining approximately 30% of its activity for 2 weeks before decreasing to near 20% at the end of one month. In contrast, the activity of the immobilized enzymes stored at room temperature decreased to less than 20% after 2 weeks and showed very little activity by the end of one month. Hence, we conclude that storage of the immobilized enzymes at 4 °C in acetate buffer is sufficient to retain the enzymatic activity for at least one month.

4. CONCLUSIONS

Although it is too early to say whether our nanotubes will wean the biofuel industry from its current limitations, or monumentally backfire, the results presented in this manuscript provide a good platform not only toward a better understanding of enzyme behavior once immobilized onto carbon nanotubes, but they might also promote further developments due to their ability to be reused several times by means of a simple magnet. Overall, it is not easy to compare the outcomes from our investigation with other pieces of work, since (1) materials, (2) enzyme immobilization strategies, and (3) assays are quite different. At the moment, we can rely only on limited sets of experiments, which include structure morphology, enzyme activity, recyclability, and storage stability, but more studies are required to fully appreciate the advantage of using this type of nanomaterial over the others.

In our study, we have proven, by using different characterization techniques (e.g., TEM, Raman analysis, ICP-OES, FTIR) and by measuring the immobilized AMG enzymatic

activity in starch substrate, that the AMG enzymes are successfully immobilized and still retain their enzymatic activity, though lower compared to the native free AMG enzyme. The reduced activity is in good relation with the circular dichroism data, as the various immobilization methods result in changes to the structural conformation of the AMG enzyme. However, the reduced enzyme activity is compensated by the ability to recycle these immobilized AMG enzymes, thereby defraying biofuel production costs in the long term. The immobilized enzymes were also shown to be able to retain their activity when stored in acetate buffer at 4 °C for at least one month. Future studies will include a higher iron oxide content in the nanotubes to favor a better hydrolytic performance of amyloglucosidase, the concurrent immobilization of AMG with other enzymes (e.g., pectinase or enzyme complexes) onto CNTs to increase biofuel production and long-term stability studies of CNT–enzyme conjugates, which will demonstrate the advantage of using CNTs for catalytic purposes in comparison with other, less durable nanomaterials.

■ ASSOCIATED CONTENT

Supporting Information

Gel Electrophoresis (SDS-Page), separation of magnetic carbon nanotubes from the starch solution for repeated usage and ICP-OES analysis. This material is available free of charge via the Internet at <http://pubs.acs.org>.

■ AUTHOR INFORMATION

Corresponding Author

*Tel +65 6516 1876. Fax: +65 6779 1554. E-mail address: phapg@nus.edu.sg.

Author Contributions

#These authors contributed equally.

Notes

The authors declare no competing financial interest.

■ ACKNOWLEDGMENTS

This research has been supported by the National University of Singapore, Department of Pharmacy ((AcRF) Tier 1-FRC grant R-148-000-129-112 and R-148-000-164-112) and by MOE of Singapore (grant MOE2009-T2-2-011, R-398-000-068-112). The author G.P. acknowledges support also by A*STAR SERC TSRP-Integrated Nano-Photo-Bio Interface grant (Project Number: 102 152 0016). The authors would like to thank Mr. Wang Hao and Dr. Ho Han Kiat's group for their assistance in SEM images and SDS-PAGE, respectively, and also Dr. Lim Fung Chye Perry for his advice on the statistical analysis.

■ ABBREVIATIONS

CNTs, carbon nanotubes; mSWCNTs, magnetic single wall carbon nanotubes; AMG, Amyloglucosidase

■ REFERENCES

- (1) Sánchez, O. J.; Cardona, C. A. Trends in biotechnological production of fuel ethanol from different feedstocks. *Bioresour. Technol.* **2008**, *99*, 5270–5295.
- (2) Nigam, P.; Singh, A. Production of liquid biofuels from renewable resources. *Prog. Energ. Combust.* **2011**, *37*, 52–52.
- (3) Fairley, P. Introduction: Next generation biofuels. *Nature* **2011**, *474*, S2–S5.

- (4) Sims, R. E. H.; Mabee, W.; Saddler, J. N.; Taylor, M. An overview of second generation biofuel technologies. *Bioresour. Technol.* **2010**, *101*, 1570–1580.
- (5) Szczesna-Antczak, M.; Kubiak, A.; Antczak, T.; Bielecki, S. Enzymatic biodiesel synthesis—Key factors affecting efficiency of the process. *Renew. Energ.* **2009**, *34*, 1185–1185.
- (6) Cang-Rong, J.; Pastorin, G. The influence of carbon nanotubes on enzyme activity and structure: investigation of different immobilization procedures through enzyme kinetics and circular dichroism studies. *Nanotechnology* **2009**, *20*, 255102.
- (7) Feng, W.; Ji, P. Enzymes immobilized on carbon nanotubes. *Biotechnol. Adv.* **2011**, *29*, 889–895.
- (8) Kim, J.; Jia, H.; Wang, P. Challenges in biocatalysis for enzyme-based biofuel cells. *Biotechnol. Adv.* **2006**, *24*, 296–308.
- (9) Silvana, A.; John, N.; Cristina, I. Nanostructured materials for enzyme immobilization and Biosensors. In *The New Frontiers of Organic and Composite Nanotechnology*; Elsevier Science: Paris, 2007.
- (10) Karajanagi, S. S.; Vertegel, A. A.; Kane, R. S.; Dordick, J. S. Structure and function of enzymes adsorbed onto single-walled carbon nanotubes. *Langmuir* **2004**, *20*, 11594–11599.
- (11) Asuri, P.; Karajanagi, S. S.; Sellitto, E.; Kim, D. Y.; Kane, R. S.; Dordick, J. S. Water-soluble carbon nanotube-enzyme conjugates as functional biocatalytic formulations. *Biotechnol. Bioeng.* **2006**, *95*, 804–811.
- (12) Pastorin, G. Crucial functionalizations of carbon nanotubes for improved drug delivery: a valuable option? *Pharm. Res.* **2009**, *26*, 746–769.
- (13) Lu, W.; Zu, M.; Byun, J. H.; Kim, B. S.; Chou, T. W. State of the art of carbon nanotube fibers: opportunities and challenges. *Adv. Mater.* **2012**, *24*, 1805–1833.
- (14) Ray, W.; Puvathingal, J. A simple procedure for removing contaminating aldehydes and peroxides from aqueous solutions of polyethylene glycols and of nonionic detergents that are based on the polyoxyethylene linkage. *Anal. Biochem.* **1985**, *146*, 307–312.
- (15) Piao, Y.; Jin, Z.; Lee, D.; Lee, H. J.; Na, H. B.; Hyeon, T.; Oh, M. K.; Kim, J.; Kim, H. S. Sensitive and high-fidelity electrochemical immunoassay using carbon nanotubes coated with enzymes and magnetic nanoparticles. *Biosens. Bioelectron.* **2011**, *26*, 3192–3199.
- (16) Hussein, L.; Urban, G.; Krüger, M. Fabrication and characterization of buckypaper-based nanostructured electrodes as a novel material for biofuel cell applications. *Phys. Chem. Chem. Phys.* **2011**, *13*, 5831–5839.
- (17) Nayak, T. R.; Jian, L.; Phua, L. C.; Ho, H. K.; Ren, Y.; Pastorin, G. Thin films of functionalized multiwalled carbon nanotubes as suitable scaffold materials for stem cells proliferation and bone formation. *ACS Nano* **2010**, *4*, 7717–7725.
- (18) Li, J.; Hong, R.; Luo, G.; Zheng, Y.; Li, H.; Wei, D. An easy approach to encapsulating Fe₃O₄ nanoparticles in multiwalled carbon nanotubes. *New Carbon Mater.* **2010**, *25*, 192–192.
- (19) Huiqun, C.; Meifang, Z.; Yaogang, L. Novel carbon nanotube iron oxide magnetic nanocomposites. *J. Magn. Magn. Mater.* **2006**, *305*, 321–321.
- (20) Qu, S.; Huang, F.; Yu, S.; Chen, G.; Kong, J. Magnetic removal of dyes from aqueous solution using multi-walled carbon nanotubes filled with Fe₂O₃ particles. *J. Hazard. Mater.* **2008**, *160*, 643–643.
- (21) Ghosh, A. K.; Naskar, A. K.; Sengupta, S. Characterisation of a xylanolytic amyloglucosidase of *Termitomyces clypeatus*. *Biochim. Biophys. Acta* **1997**, *1339*, 289–296.
- (22) Sunao, Y.; Noriyuki, S.; Kiyoshi, O.; Mitsuo, S.; Yuji, O. Enzymatic Hydrolysis and Ethanol Fermentation of By-Products from Potato Processing Plants. *Food Sci. Technol. Res.* **2009**, *15*, 653–658.
- (23) Erdei, B.; Barta, Z.; Sipos, B.; Réczey, K.; Galbe, M.; Zacchi, G. Ethanol production from mixtures of wheat straw and wheat meal. *Biotechnol. Biofuels* **2010**, *3*, 16.
- (24) Kim, C.; Lee, G.; Abidin, Z.; Han, M.; Rhee, S. Immobilization of *Zymomonas mobilis* and amyloglucosidase for ethanol production from sago starch. *Enzyme Microb. Technol.* **1988**, *10*, 426–430.
- (25) del Pozo-Insfran, D.; Urias-Lugo, D.; Hernandez-Brenes, C.; Serna Saldívar, S. O. Effect of Amyloglucosidase on Wort Composition and Fermentable Carbohydrate Depletion in Sorghum Lager Beers. *J. Inst. Brew.* **2004**, *110*, 124–132.
- (26) Fuwa, H. A new method for microdetermination of amylase activity by the use of amylose as the substrate. *J. Biochem.* **1954**, *41*, 583–583.
- (27) Xiao, Z.; Storms, R.; Tsang, A. A quantitative starch-iodine method for measuring alpha-amylase and glucoamylase activities. *Anal. Biochem.* **2006**, *351*, 146–146.
- (28) Busto, M. N.; Ortega, N.; Perez-Mateos, M. Effect of immobilization on the stability of bacterial and fungal β -d-glucosidase. *Process Biochem.* **1997**, *32*, 441–449.
- (29) Mayo, S. L.; Olafson, B. D.; Goddard, W. A. DREIDING: a generic force field for molecular simulations. *J. Phys. Chem.* **1990**, *94*, 8897–8909.
- (30) Jenny, E.; Lo, G. Comparison between different inorganic supports for the immobilization of amyloglucosidase and α -amylase to be used in enzyme reactors in flow-injection systems: Part I. Hydrolysis of maltose, maltooligosaccharides and soluble starch. *Anal. Chim. Acta* **1993**, *276*, 303–318.
- (31) Matsuura, K.; Saito, T.; Okazaki, T.; Ohshima, S.; Yumura, M.; Iijima, S. Selectivity of water-soluble proteins in single-walled carbon nanotube dispersions. *Chem. Phys. Lett.* **2006**, *429*, 497–502.
- (32) Gao, Y.; Kyrtzsis, I. Covalent Immobilization of Proteins on Carbon Nanotubes Using the Cross-Linker 1-Ethyl-3-(3-dimethylaminopropyl)carbodiimide—a Critical Assessment. *Bioconjugate Chem.* **2008**, *19*, 1945–1950.
- (33) Jiang, Y.; Guo, C.; Xia, H.; Mahmood, I.; Liu, C.; Liu, H. Magnetic nanoparticles supported ionic liquids for lipase immobilization: Enzyme activity in catalyzing esterification. *J. Mol. Catal. B: Enzym.* **2009**, *58*, 103–109.
- (34) Moriyama, K.; Sung, K.; Goto, M.; Kamiya, N. Immobilization of alkaline phosphatase on magnetic particles by site-specific and covalent cross-linking catalyzed by microbial transglutaminase. *J. Biosci. Bioeng.* **2011**, *111*, 650–653.
- (35) Yadav, S.; Kumar, A.; Pundir, C. S. Amperometric creatinine biosensor based on covalently coimmobilized enzymes onto carboxylated multiwalled carbon nanotubes/polyaniline composite film. *Anal. Biochem.* **2011**, *419*, 277–283.
- (36) Duangkamon, B.; Wannapong, T.; Darapond, T. Encapsulation of TiO₂ nanoparticles into single-walled carbon nanotubes. *New J. Phys.* **2009**, *11*, 093011.
- (37) Cox, B. J.; Thamwattana, N.; Hill, J. M. Mechanics of Atoms and Fullerenes in Single-Walled Carbon Nanotubes. I. Acceptance and Suction Energies. *Proc. R. Soc. London, Ser. A* **2007**, *463*, 461–476.
- (38) Hu, F.; Chen, S.; Wang, C.; Yuan, R.; Chai, Y.; Xiang, Y.; Wang, C. ZnO nanoparticle and multiwalled carbon nanotubes for glucose oxidase direct electron transfer and electrocatalytic activity investigation. *J. Mol. Catal. B: Enzym.* **2011**, *72*, 298–304.
- (39) Konwarh, R.; Kalita, D.; Mahanta, C.; Mandal, M.; Karak, N. Magnetically recyclable, antimicrobial, and catalytically enhanced polymer-assisted “green” nanosystem-immobilized *Aspergillus niger* amyloglucosidase. *Appl. Microbiol. Biotechnol.* **2010**, *87*, 1983–1992.
- (40) Souza Filho, A. G.; Chou, S. G.; Samsonidze, G. G.; Dresselhaus, G.; Dresselhaus, M. S.; Lei An, J. L.; Swan, A. K.; Unlu, M. S.; Goldberg, B. B.; Jorio, A.; Gruneis, A.; Saito, R. Stokes and anti-Stokes Raman spectra of small-diameter isolated carbon nanotubes. *Phys. Rev. B* **2004**, *69*, 115428.
- (41) Fantini, C.; Jorio, A.; Souza, M.; Strano, M. S.; Dresselhaus, M. S.; Pimenta, M. A. Optical transition energies for carbon nanotubes from resonant Raman spectroscopy: environment and temperature effects. *Phys. Rev. Lett.* **2004**, *93*, 147406.
- (42) Gupta, P.; Mishra, S.; Chaudhuri, T. K. Reduced stability and enhanced surface hydrophobicity drive the binding of apo-aconitase with GroEL during chaperone assisted refolding. *Int. J. Biochem. Cell Biol.* **2010**, *42*, 683–692.
- (43) Seinosuke, U. Fungal glucoamylases and raw starch digestion. *Trends Biochem. Sci.* **1981**, *6*, 89–90.